SCIENCE CHINA
Information Sciences

• LETTER •

April 2025, Vol. 68, Iss. 4, 149404:1–149404:2
https://doi.org/10.1007/s11432-024-4318-6

Analysis and fabrication of a SiC super-junction termination structure in a state of charge imbalance

Haobo KANG[1†], Fengyu DU[1†], Hao YUAN[1*], Boyi BAI[1], Yu ZHOU[1], Jingyu LI[1], Chao HAN[1,2], Xiaoyan TANG[1], Qingwen SONG[1,2] & Yuming ZHANG[1,2]

[1] *Key Lab of Wide Band Gap Semiconductor Materials and Devices, School of Microelectronics, Xidian University, Xi'an 710071, China*
[2] *Xidian-Wuhu Research Institute, Wuhu 241000, China*

Received 18 October 2024/Revised 4 December 2024/Accepted 19 February 2025/Published online 12 March 2025

Citation Kang H B, Du F Y, Yuan H, et al. Analysis and fabrication of a SiC super-junction termination structure in a state of charge imbalance. Sci China Inf Sci, 2025, 68(4): 149404, https://doi.org/10.1007/s11432-024-4318-6

A qualified termination should have the same blocking capability as an active region to prevent a super-junction (SJ) device from breaking down prematurely. The 960 V [1] and 1920 V [2] SiC SJ terminations using "trench etching-sidewall ion implantation" are being investigated. However, their termination efficiencies (experimental value/active simulated value) are only 63.2% and 76.8%, respectively, which are much lower than the ideal value. The most obvious difference between the termination and the active region is that the surface potential of each SJ structure is not equal, which seriously affects the blocking ability of the termination. The BV of the Si SJ termination reached an optimal state under charge imbalance, a discovery that was established with an analytical model [3]. Nevertheless, no systematic analysis is provided, and it is not verified in SiC SJ devices, either. To solve the issue, a SiC SJ JBS with a charge imbalance termination structure is fabricated by the "two epitaxy-channel implantation" process.

Simulation and analysis. The schematic of the SiC SJ termination is shown in Figure 1(a). In the active and transition regions, the depth and width of the p-pillar and n-pillar are 4 and 2 μm, respectively. The n-pillar is 6×10^{16} cm^{-3} of uniform doping concentration, and the p-pillar is prepared by the channel implanting of nearly uniform 6×10^{16} cm^{-3} (after being compensated).

The total thickness of the epitaxy layer is 4.5 μm. In the termination, the width of the p-pillar (Wp) is set as 2 μm, but the width of the n-pillar (Wn) becomes a variable parameter (from 1.1 to 2 μm). A 0.35 μm deep p+ structure is designed at the top of the p-pillar to relieve electric field (EF) crowding at the surface, which does not damage the blocking performance of the device. The simulated BV (by Sentaurus of technology computer aided design) of the cell is 915 V (current criterion), and 18 p-pillars are applied in the termination simulation. The smaller the Wn in the termination is, the more p-pillars that need to be depleted, leading to a larger termination area in Figures 1(c)–(e). The simulated result of BV vs. Wn in the termination is shown in Figure 1(b). The BV reaches a maximum value of 860 V when the Wn is 1.1 and 1.3 μm.

The EF distribution for termination with a Wn of 0.7, 1.1, and 2 μm at the moment of breakdown is displayed in Figures 1(c)–(e). The surface potential distribution of three types of terminations is extracted in Figure 1(f). As the Wn decreases from 2 to 0.7 μm, the rising rate of the surface potential gradually decreases, and the number of termination p-pillars required to be depleted would also increase at the same time.

The EF distribution at the p+ corner (A-A′) and the bottom of the p-pillar (B-B′) is extracted in the direction of the X-axis in Figures 1(h), (j), and (l), and the EF distribution along the midline of the first to the fifth p-pillar (C-C′) (D-D′) (E-E′) (F-F′) (G-G′) is extracted vertically in Figures 1(g), (i), and (k).

Figure 1(g) shows that the SJ termination is in a state of charge balance because the slope of the EF along the p-pillar midline is nearly 0, which is the same as the active region. However, the EF peak value at the p+ corner (E_{top} = 3.51 MV/cm) is higher than the one at the bottom of the p-pillar (E_{bottom} = 1.7 MV/cm) under this condition in Figure 1(h), which demonstrates that premature breakdown occurs easily, and a BV of 494 V is achieved. Combined with Figure 1(f), that phenomenon is attributable to the unequal surface potential of each SJ in the termination, which gradually weakens the offset effect of the EF at the current p+ caused by the later p+, leading to EF crowding at the first p+ corner.

From Figure 1(i), the slope of EF along the p-pillar midline is positive, which indicates that the SJ termination is in a state of p-pillar overcompensation with a Wn of 1.1 μm. In Figure 1(j), the EF peak value at the p+ corner is equal to the one at the bottom of the p-pillar ($E_{\text{top}} = E_{\text{bottom}}$

* Corresponding author (email: haoyuan@xidian.edu.cn)
† These authors contributed equally to this work.

© Science China Press 2025

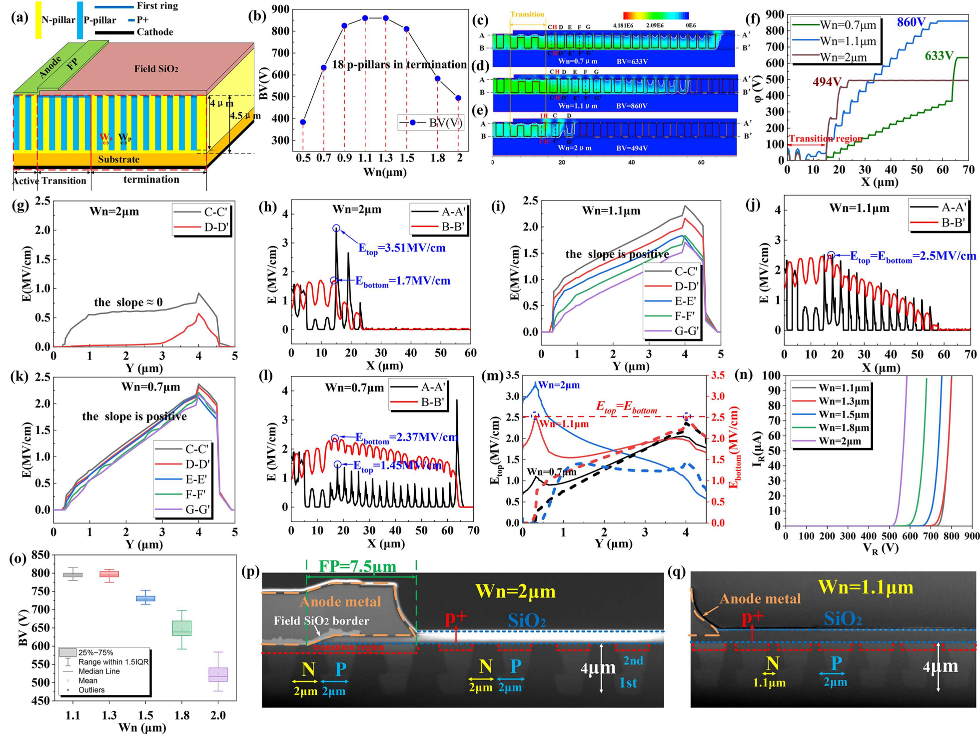

Figure 1 (Color online) (a) Schematic of the SiC SJ termination. (b) The simulated change profile to BV vs Wn. The 2-D EF distribution of the termination with Wn = (c) 0.7 μm, (d) 1.1 μm, and (e) 2 μm. (f) The 1-D surface potential distribution of three terminations. The 1-D EF Wn= (h) 2 μm, (j) 1.1 μm, (l) 0.7 μm lateral and Wn = (g) 2 μm, (i) 1.1 μm, (k) 0.7 μm longitudinal (along the midline of the p-pillar) distribution of the termination. (m) The 1-D EF longitudinal distribution across the first p+ corner ((c) H-H′, (d) H-H′, (e) H-H′) and the bottom of the p-pillar ((c) C-C′, (d) C-C′, (e) I-I′) for the three terminations. (n) Measured reverse characteristics. (o) The BV statistic box distribution of SJ JBS with a Wn from 1.1 to 2 μm. Cross-sectional SEM images of the SJ termination with a Wn of (p) 2 μm and (q) 1.1 μm.

= 2.5 MV/cm). Correspondingly, the BV is at a maximum value of 860 V. Therefore, the BV of the SJ termination is optimum in the situation of charge imbalance.

However, if the Wn is too narrow (0.7 μm), it will place the p-pillars in a serious state of overcompensation in Figure 1(k). As a result, the EF peak value at the bottom of the p-pillar (E_{bottom} = 2.37 MV/cm) is higher than the one at the p+ corner (E_{top} = 1.45 MV/cm) in Figure 1(l). Under this condition, the premature breakdown is caused by the EF crowding at the last p+ corner because of insufficient p-pillars set in the simulation, obtaining a BV of only 633 V.

In Figure 1(m), as the Wn gradually decreases from 2 to 0.7 μm, the slope of EF gradually increases because of the p-pillar overcompensation, which lowers the peak of EF at the p+ corner and also raises it at the bottom of the p-pillar. Both the EF peak of the p+ corner and the bottom of the p-pillar reach the critical value when Wn = 1.1 μm.

Experiment and fabrication. The 2.5 μm SiC epitaxy layer is grown uniformly on the 4H-SiC substrate. The SJ p-pillars are created utilizing a combination of five random Al implantations and one channel Al implantation in [0001] direction. The aforementioned processes are repeated twice to form the drift region (4.5 μm) and the p-pillars (4 μm) in depth. Then, the wafer will be annealed in Ar atmosphere at 1700°C for 10 min to repair the lattice damages and activate the implanted ions. The rest of the steps are carried out following a standard SiC JBS preparation process. The cross-section of SEM images of the SJ termination with a Wn of 2 and 1.1 μm are shown in Figures 1(p) and (q). The length of the field plate is 7.5 μm in Figure 1(p). It can accelerate the depletion of pn-pillars and relieve the crowding of EF at the corner of the transition region p+.

The reverse breakdown profiles and the statistical results of BV with a Wn of 1.1–2 μm are shown in Figures 1(n) and (o). The average value of their BV is 800 V (Wn = 1.1 and 1.3 μm, Wp = 2 μm). Then, the BV decreases as the Wn increases, a trend that is consistent with the simulation.

Conclusion. The charge imbalance termination in the SiC SJ JBS is verified. Different from the active region, the BV of the SJ termination reaches a maximum value in a state of p-pillar overcompensation. The Wn is smaller than Wp in the termination, and the EF peaks at the p+ corner and the bottom of the p-pillar reach the critical value simultaneously. The results of the experiment are consistent with the simulation, confirming the correctness of the proposed design method. The termination efficiency is up to 87%.

Acknowledgements This work was supported by National Key R&D Program of China (Grant No. 2021YFB3601800) and Hefei Comprehensive National ScienceCenter.

References

1 Wang H, Wang C, Wang B, et al. Hybrid termination with wide trench for 4H-SiC super-junction devices. IEEE Electron Dev Lett, 2021, 42: 216–219
2 Wang B, Wang H, Wang C, et al. Design and fabrication of 1.92 kV 4H-SiC super-junction SBD with wide-trench termination. IEEE Trans Electron Dev, 2021, 68: 5674–5681
3 Qian Q, Sun W, Zhu J, et al. A novel charge-imbalance termination for trench superjunction VDMOS. IEEE Electron Dev Lett, 2010, 31: 1434–1436